EXPERIMENTAL CHARACTERIZATION AND MODELING OF HELIUM DISPERSION IN A ¼-SCALE TWO-CAR RESIDENTIAL GARAGE

Pitts, W.M., Prasad, K., Yang, J.C., and Fernandez, M.G.
[1] 100 Bureau DR, National Institute of Standards and Technology, Gaithersburg, MD, 20899, USA, wpitts@nist.gov, kprasad@nist.gov, jiann.yang@nist.gov, Marco.Fernandez@nist.gov

ABSTRACT

A series of experiments are described in which helium was released at a constant rate into a 1.5 m × 1.5 m × 0.75 m enclosure designed as a ¼-scale model of a two car garage. The purpose was to provide reference data sets for testing and validating computational fluid dynamics (CFD) models and to experimentally characterize the effects of a number of variables on the mixing behavior within an enclosure and the exchange of helium with the surroundings. Helium was used as a surrogate for hydrogen, and the total volume released was scaled as the amount that would be released by a typical hydrogen fueled automobile with a full tank. Temporal profiles of helium were measured at seven vertical locations within the enclosure during and following one hour and four hour releases. Idealized vents in one wall sized to provide air exchange rates typical of actual garages were used. The effects of vent size, number, and location were investigated using three different vent combinations. The dependence on leak location was considered by releasing helium from three different points within the enclosure. It is shown that the National Institute of Standards and Technology (NIST) CFD code Fire Dynamics Simulator (FDS) provides time resolved predictions for helium concentrations that agree well with the experimental measurements.

1.0 INTRODUCTION

1.1 Background

Concerns about global warming are driving efforts to develop hydrogen powered systems as replacements for many current applications utilizing hydrocarbon fuels. A number of demonstrations are underway that are designed to show that hydrogen can be used for mobile and stationary applications. The ultimate goal is to develop a hydrogen-based economy.

The physical properties of hydrogen differ from those for hydrocarbon fuels. As a result, the mixing and combustion behaviors of hydrogen differ in significant ways from hydrocarbons and must be taken into account when engineering systems for safe operation and fire prevention. Efforts are underway to develop standards and codes appropriate for hydrogen fueled systems. The differences between hydrogen and typical hydrocarbon fuels are particularly important when hydrogen is released into enclosed spaces such as building, garages, and tunnels. Example applications include hydrogen fueled automobiles parked in residential garages and stationary fuel cells located within a building.

1.2 Previous Work

The unique fire safety problems associated with hydrogen have led to a number of studies aimed at experimentally characterizing the temporal mixing behaviors of hydrogen releases within enclosures as well as the application of flow models for predicting these behaviors. One of the earliest studies was performed by Koontz et al. who measured the temporal behavior of hydrogen concentrations at six locations within a two-car garage following hydrogen release near the floor or generation during the charging of a battery. [1] Swain et al. used a computational fluid dynamics (CFD) code to simulate these experiments and validate the modeling. [2]

Many researchers have been reluctant to use hydrogen for experimental testing due to safety concerns. It has been common to use helium instead as a surrogate. The density of helium is twice as large and its molecular diffusion coefficient is roughly 90 % of hydrogen. Swain et al. investigated the differences between helium and hydrogen releases using a CFD approach validated by comparison with helium measurements [3] Time resolved helium concentration measurements in a ½-scale corridor equipped with various types of vents in which helium was released were shown to agree well with CFD predictions. Swain et al. later provided more detailed comparisons of predicted time-resolved helium and hydrogen distributions during releases into enclosures. [4]

In an unpublished contractor report Swain described time-resolved helium measurements at four locations within a full-scale single car garage. [5] The helium was released from underneath a wooden mock-up of an automobile. Limited CFD modeling of the helium releases agreed well with the experimental measurements. Papanikolaou and Venetsanos used a CFD model to simulate the Swain results in more detail. [6] In 2001 Breitung et al. reported a CFD analysis of short pulses of hydrogen released from an automobile parked inside a single-car garage with two vents near the ceiling. [7]

A variety of CFD codes for modeling hydrogen dispersion were tested in a round robin study involving twelve laboratories [8] that simulated hydrogen concentrations measured at six locations along the vertical direction of a large sealed cylindrical vessel by Shebeko et al. [9]. There were substantial variations in calculated hydrogen concentrations at various times for the different models. The calculated values generally clustered about the experimental values within a range of 0.5 to 2. In a few cases, the calculated values were more than a factor of 10 lower.

During the Second International Conference on Hydrogen Safety, a number of papers reported experimental findings on the release and dispersion of helium [10] or hydrogen [11,12,13] in real-scale enclosures representative of garages. Gupta et al. [10] and Lacome et al. [11] utilized enclosures with small openings near the base to minimize pressure differences between the inside and outside of the enclosure, while limiting the loss of injected gas. Both groups reported real-time concentration measurements at multiple locations. Injected gas volume flow rates and durations were varied. Tchouvelev et al. studied hydrogen released into an enclosure containing a fan for mixing. [12] Ishimoto et al. considered releases of hydrogen into a ventilated enclosure. [13]

One of the experiments described by Lacome et al. [11] served as the basis for a second round robin study of CFD capabilities. [14] The calculations were run prior to the availability of the experimental results, i.e., a blind test, and then repeated afterwards. As found earlier [8], there were significant differences between the experimental hydrogen concentration measurements and the CFD predicted values at various times. The magnitudes of the differences were similar, with calculated values generally falling within a range of 0.5 to 2 of the experimental values. For the worst case in the blind test outliers fell in a range of 0 to 2.7. The largest differences were for sensors located in the lower part of the enclosure and along the centerline of the buoyant flow. The gaps between the experimental and calculated concentrations were reduced somewhat for calculations made after the experimental data were available, but significant differences remained.

Zhang et al. describe the application of one of the CFD models included in the round robin [14] to the Lacome et al. data [11] in a separate manuscript. [15] The agreement between the CFD and experimental results appears to be somewhat better than indicated in the round robin paper. Tchouvelev et al. applied CFD calculations to their measurements of hydrogen in a chamber with fan-assisted mixing. [12] The temporal variations in hydrogen concentrations at the various measurement locations were captured well.

Barley et al. describe CFD modeling of hydrogen dispersion in real-scale garages with a goal of understanding and assessing the effectiveness of passive ventilation openings for removing released hydrogen. [16] They found that two openings near the top and bottom of the enclosure are most effective due to the resulting buoyancy-induced flow. Barley et al. also describe a simple analytical model for predicting flow in and out of the enclosure based on the hydrostatic pressure differences across the enclosure boundary due to low density hydrogen and include a factor to capture the effects of stratification. The analytical model agreed well with the CFD predictions for reasonable values of the stratification factor. Zhang et al. also discuss an analytical approach for predicting hydrogen distributions in an enclosure based on induced hydrostatic pressure differences. [15] Their model is modified from a two zone model commonly used for enclosure fires that assumes an upper layer of uniformly mixed gases and a lower air layer. Significant differences between predictions and experiment results were attributed to density gradients presence in the upper layer of the experiment.

1.3 Fire Dynamics Simulator (FDS)

FDS is a large-eddy simulation (LES) model for fire behavior that has been under development at the National Institute of Standards and Technology for several years. [17] The equations and algorithms are specially formulated to describe buoyancy induced flows. The code has been extensively tested and validated and is widely used in the fire research and engineering communities.

FDS should provide an effective approach for predicting the mixing and dispersion behavior for low density gases such as helium and hydrogen when released into an enclosure. FDS was one of the models used in the CFD round robin based on the Lacome et al. data. [11] According to the report, FDS significantly overestimated the experimental hydrogen concentrations when the default value of C_s = 0.2 was used for the Smagorinski constant, a parameter related to the degree of small-scale turbulent mixing not resolved by the model, and provided much better agreement in the post-test modeling when C_s was reduced to 0.12. The CFD results described in [15] are also based on FDS.

1.4 Problem Description

As hydrogen-powered automobiles come on to the market, it is likely that they will be parked in the existing stock of residential garages. For this reason, it is important to understand the implications of potential hydrogen leaks in typical residential garages. Even though the literature described above is focused on garages, many of the studies have not fully investigated parameters likely to be important in actual garages. Two such parameters are hydrogen leak location and the size and spatial distribution of leaks. Investigations focused on losses of hydrogen from an enclosure during and following a release are limited.

Leak rates for garages are typically described in terms of the number of air changes per hour (*ACH*) for an enclosure of volume, V_{enc}, which corresponds to a volume flow exchange rate across the enclosure boundary, Q_{enc}, given by $Q_{enc} = V_{enc} \times ACH/3600$. *ACH* can vary substantially with time and depends not only on the areas of openings connecting across the enclosure boundary, but also on such factors as weather conditions and forced ventilation. Values of Q_{enc} can be related to an effective leak area, *ELA* by use of the Bernoulli equation,

$$ELA_H = (Q_{enc})_H/(2 \times \Delta P/\rho)^{1/2}, \quad (1)$$

where the subscript H indicates evaluation at a specific pressure difference ΔP between the interior and exterior and gas density ρ. A value of H = 4 Pa is often taken to be representative of pressure difference across a garage boundary. [18] Note that ELA_H does not normally correspond to the actual open area in a garage boundary since experimental flow rates are typically [18] given by

$$Q_{enc} = C \times \Delta P^n, \quad (2)$$

where C is the flow parameter and n is an experimental parameter that varies between 0.5 and 1.

Studies indicate that values of ACH and $ELA_{4\ Pa}$ vary widely for garages in the United States, e.g., see [18,19]. For testing purposes, it is reasonable to consider ACHs on the low side of those observed. For this purpose, a recommended minimum value of Q_{enc} = 2.73 m^3/min (100 ft^3/min) per stored automobile included in an early version of an American Society of Heating Refrigeration, and Air Conditioning Engineers (ASHRAE) standard was used. [20] Swain et al. referred to this value in an earlier study. [2] Note that this recommendation is no longer included in current versions of the ASHRAE standard, but is incorporated in the 2009 International Mechanical Code published by the International Code Council. [21] A simple calculation reveals that this value corresponds exactly to an $ACH = 3\ h^{-1}$ for a single car garage sized 3.048 m (w) × 6.096 m (l) × 3.048 m (h) (10 ft × 20 ft × 10 ft). On this basis, an $ACH = 3\ h^{-1}$ was adopted as a representative lower value for this study.

The purpose of the current study is twofold. The first is to provide a set of reference data for testing and validating the capability of FDS and other CFD codes to predict the concentration distributions within an enclosure, including losses to the ambient surroundings, of a buoyant gas during release and post-release periods. The second is to experimentally characterize the effects of the gas release point, the buoyant gas release rate, and the vent size(s) and location(s) on the mixing behavior and interior concentration profiles during the release and post-release periods.

For modeling purposes it is desirable to have accurate, repeatable experiments with well defined boundary conditions and initial conditions. Such control is exceedingly difficult in actual garages, which are subject to outside weather conditions (i.e., changing winds and temperatures) and have leaks that are difficult to characterize. The choice was made to perform measurements in a well controlled laboratory environment. In order to maintain the test facility at a manageable size and limit the amount of buoyant gas required, a scaled enclosure is used. Simple vent configurations, single and double vents located in a single wall, are used for the initial measurements.

It should be noted that the reduced-scale experiments are not designed to provide a full similitude model of a full-scale garage. Due to the nature of the system, it is not possible to match all of the dimensionless numbers expected to be important. The experiment is designed such that spatial scales, gas volume flow rates, and flow times are scaled to match those expected in a full-scale experiment.

2.0 EXPERIMENTAL AND COMPUTATIONAL DESCRIPTIONS

The reduced-scale experiment is based on the following highly idealized scenario. A release of 5 kg of hydrogen (representative of a full tank on current designs of hydrogen powered automobiles) occurs at room temperature within a two-car garage having interior dimensions of 6.096 m × 6.096 m × 3.048 m. The hydrogen is completely released at a constant rate over one hour or four hours at a fixed location within the garage.

A physical scale model having interior dimensions of 1.5 m × 1.5 m × 0.75 m was constructed from nominally 1.27 cm thick poly(methyl methacrylate) sheets. The corresponding scaling factor is 0.246. Five pieces of the acrylate were glued together to form a sealed enclosure with an open front end. A 2.54 cm wide flange was attached around the outside edge of the open end, and a 1.576 m × 0.818 m removable front face was placed over the flange and held in place with a series of clamps. A neoprene gasket and stopcock grease were used to form a tight seal between the front face and flange. Figure 1 shows a schematic for the enclosure along with a photograph.

All vents, a pressure tap, and electrical and gas feedthroughs were incorporated into the removable front faces. Three faces were fabricated. The first had a single 2.40 cm ± 0.02 cm square (5.76 cm^2 area) opening at the center of the face. This size was determined using Eq. (1) to estimate the area required for $ACH = 3\ h^{-1}$ ($Q_{enc} = 1.41 \times 10^{-3}\ m^3/s$) with ΔP = 4 Pa (actual calculated area is 5.46 cm^2). Subsequent measurements (described below) with this face in place provided the parameters (C = 4.45

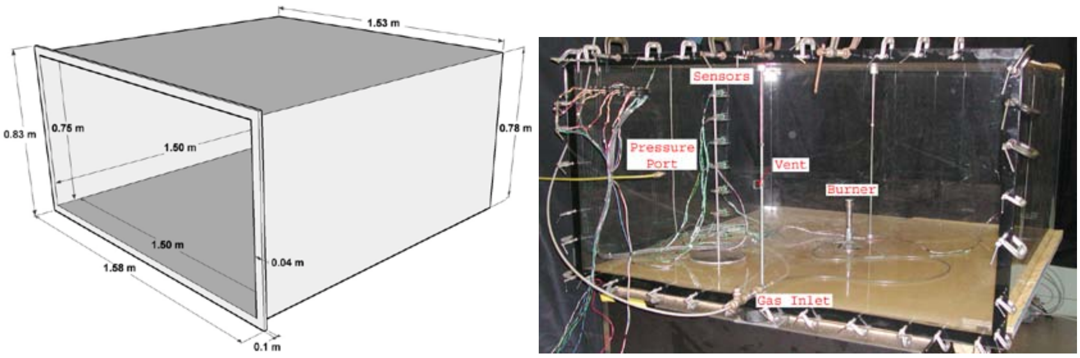

Figure 1. A schematic and photograph of the ¼-scale two car garage are shown.

$\times 10^{-4}$ $m^3/(sPa^n)$, $n = 0.531$) for use in Eq. (2). The $Q_{enc} = 9.28 \times 10^{-4}$ m^3/s calculated is 62 % of the value based on Eq. (1). A second face was prepared with the vent area increased by a factor of 1.60, i.e., a square with 3.05 cm ± 0.02 cm sides (9.3 cm^2 area). Two equal square vents with 2.15 cm ± 0.02 cm sides (total area = 9.25 cm^2) were placed in the third face equal distances from the sidewalls with the bottom edge of the lower 2.54 cm above the floor and the top edge of the upper located 2.54 cm below the ceiling. Experimental measurements with this front face (see below) yielded $C = 7.371 \times 10^{-4}$ $m^3/(sPa^n)$ and $n = 0.484$, corresponding to $Q_{enc} = 1.44 \times 10^{-3}$ m^3/s for $\Delta P = 4$ Pa. This is close to the desired value of 1.41×10^{-3} m^3/s for $ACH = 3$ h^{-1}.

Due to safety concerns, helium was chosen as the buoyant gas for this study. A mass flow controller was used to deliver constant volume flow rates chosen such that the total volume of helium delivered during the release period (either 3600 s or 14,400 s) corresponded to the dimensionally scaled volume (59.8 m^3) for a release of 5 kg of hydrogen into the full-scale garage. The corresponding volume of 0.890 m^3 for the reduced-scale garage yields flow volume rates of 2.47×10^{-4} m^3/s = 14.8 L/min and 6.18×10^{-5} m^3/s = 3.71 L/min for the one hour and four hour releases, respectively. The actual volume flow rates delivered by the mass flow controller were measured to be 14.95 L/min and 3.74 L/min using a Gilabrator-2 electronic bubble flow meter from Gilian (Note: Certain commercial equipment, instruments, or materials are identified in this paper in order to adequately specify the experimental procedure. Such identification does not imply recommendation or endorsement by the National Institute of Standards and Technology, nor does it imply that the materials or equipment are necessarily the best available for the purpose.) In an unpublished report, Mulholland and Fernandez found the expanded uncertainty (2σ) for this instrument to be 1.8 %. [22]

The helium flowed by way of tubing through a feedthrough into the enclosure where it was released from a Fischer burner, chosen as a convenient means to release helium over an area, with a $D_o = 3.6$ cm diameter circular opening located 20.7 cm above its base. The burner exit was located at one of three locations: on the floor at the center of the enclosure (0.75 m, 0.75 m, 0.207 m) on the floor at the center of the rear wall with the exit edge 3.0 cm from the wall (0.75 m, 1.45 m, 0.207 m), and raised at the center of the enclosure with the burner exit located 2.5 cm below the ceiling (0.75 m, 0.75 m, 0.725 m). Coordinates are given relative to an origin located on the floor at the front of the enclosure on the left-hand edge. Laboratory and gas temperatures were maintained at 21 ºC ± 1 ºC.

The average helium flow velocities, U_o, at the flow exit are 0.245 m/s and 0.061 m/s for the one hour and four releases, respectively. Following Chen and Rodi [23], for the higher flow velocity, the exit Reynolds number, Re, and Froude number, Fr, given by

$$\mathrm{Re} = \rho_{He} D_o / \nu_{He}, \quad \mathrm{Fr} = (\rho_{He} U_o^2)/(g D_o(\rho_{air} - \rho_{He})), \tag{3}$$

where v is the kinematic viscosity and g the gravitational constant, are Re = 75 and Fr= 0.0273. The Reynolds number indicates the initial flow is laminar and, based on criteria given by Chen and Rodi [23], becomes buoyancy dominated approximately 2 cm above the flow exit. The four hour velocity flow will become buoyancy dominated even closer to the exit.

Measurements recorded during an experiment include helium volume fractions at seven locations along a vertical line located 37.5 cm from the left and front walls. The heights of the sensors were #1: 9.3 cm, #2: 18.5 cm, #3: 27.6 cm, #4: 37.2 cm, #5: 46.6 cm, #6: 55.9 cm, and #7: 65.0 cm. An eighth sensor was moved to variable positions during different tests to check the horizontal uniformity of the helium distribution within the enclosure. Two types of helium sensors were used: Neodym Industries Panterra hydrogen sensors and Xensor Integration Model TCG-3880Pt sensors. Both models respond to variations in the gas thermal conductivity as the helium concentration changes. Each sensor was individually calibrated in-house using a computer-controlled mixing system. [24] The helium volume fractions generated by the calibration system were measured with 1 % uncertainty by a pair of Siemens Calomat 6 7MB2527 gas analyzers. Individual calibration curves were generated by fitting polynomials to plots of helium volume fraction versus sensor output voltage. Helium volume fractions recorded by the two sensor models during repeated helium release experiments agreed very well. Due to ease of use and a somewhat smaller sensor size, all of the measurements reported here were taken using Xensor Integration probes.

A single pressure port was located on the front face at a location 37.5 cm from the left wall and 37.5 cm above the floor. The differential pressures between the enclosure interior and ambient surroundings was measured by a calibrated 133 Pa (1 torr) Baratron electronic manometer.

The voltages generated by the concentration and pressure transducers were digitized using a combination of National Instruments digitizer and Labview software. Voltages were digitized at a 2 kHz rate and then averaged over either 1 s or 10 s before being saved in a file along with the relative time of the sample. Both sampling rates could be employed during an experiment, with the time for the change from 1 s to 10 s averaging determined by the user. Data was provided as comma delimited files. Conversion of the measured voltage values to volume fractions and pressures along with data plotting was accomplished by importing the voltages into SigmaPlot software and using specially written data transforms to implement the individual calibration curves.

A typical helium release experiment consisted of recording a short background level before initiating the helium flow, starting the helium flow appropriate for a one hour or four hour release, halting the helium flow at the appropriate time, and recording the pressure and concentration sensor voltages for variable periods (sometimes up to several days) during the post release period. Measurements during the release phase were always recorded with the 1 s averaging time, while it was common to switch to the 10 s average sometime during the post release period to limit the number of samples recorded.

In order to characterize the vents used during the experiments, tests comparable to the "fan pressurization test" used to measure leaks in actual buildings were performed. [18,19] In this test a fan generates a flow that either enters or exits the enclosure. The pressure change due to the flow is recorded as a function of the flow volume generated by the fan, and the results are fit to an expression similar to Eq. (2). Results are then used to calculate such parameters as ELA_H. We simulated a fan pressurization test by passing known volume flow rates of house air through the Fischer burner and measuring the resulting differential pressure between the enclosure interior and ambient laboratory.

FDS calculations were run on selected cases based on the experiments. These calculations are described in more detail elsewhere. [25] The production version of FDS available at NIST at the time, Version 5.2.0, was used for the calculations discussed here. The only modification made to the code was to use the calculated value of helium molecular diffusion in air in place of the turbulent diffusion coefficient when its value was larger. This modification only had minor effects on the predicted

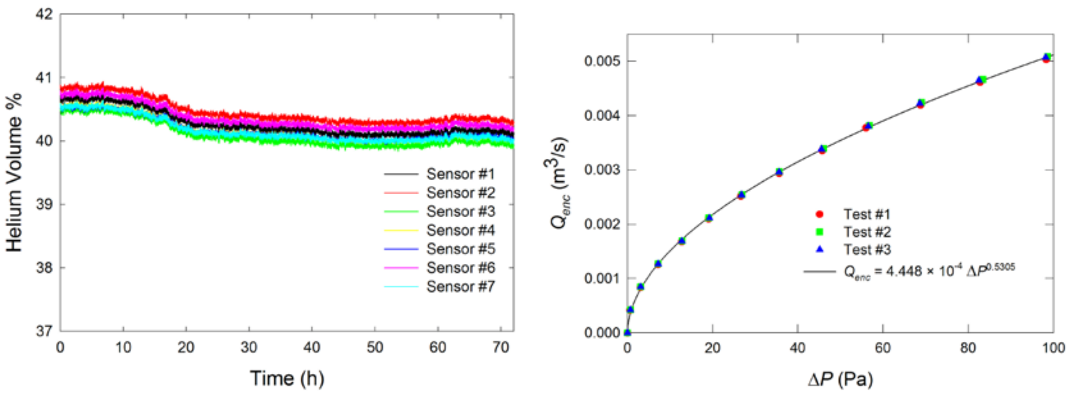

Figure 2. Results for an enclosure helium leak test (left) and a fan test (right) are shown.

results. Note that the FDS User's Manual recommended value of Smagorinski constant, $C_s = 0.2$, was employed. Additional details concerning gridding and boundary conditions are available in [25].

3. RESULTS

Figure 2 shows examples of tests used to characterize the enclosure. The plot on the left is the result of a leak test in which the vent was sealed following a one hour helium release. Less than one percent of the helium was lost over a three-day period. Checks with a helium leak detector showed small amounts of helium escaping from the plug used for the vent, around the electrical feed throughs, and along a short section of the flange seal to the enclosure. Differential pressure measurements during the test showed the pressure responding to atmospheric pressure changes, but not fully tracking the atmospheric pressure due to the small leaks. The slightly different helium volume fraction values seen in Figure 2 are representative of the calibration differences between individual sensors. The plot on the right is the result of a fan test with the 2.40 cm square opening in the front face. Values of Q_{enc} are plotted against ΔP, and the solid line is the result of a fit to Eq. (2). Eighteen combinations of release time (2), release point (3), and vent type (3) were studied. Examples of the results are shown to provide indications of the effects of the parameters on observed mixing behavior. Measurements taken at various locations within the enclosure indicated that variations in helium volume fraction in a given horizontal plane were generally much smaller than differences observed between any two adjacent vertical sensors.

Figure 3 compares temporal helium concentration curves measured at seven measurement heights for four hour helium releases at the center of the enclosure near the floor for the two single vent areas. The curves show that the relatively small concentration gradients that develop during the release period begin to dissipate during the post release period. The maximum helium volume fraction is slightly larger and the vertical concentration gradients are reduced during the release and post release periods for the experiment with the smaller vent. During the post release period helium concentrations decay faster for the enclosure with the larger vent. At longer times than shown in Figure 3, the concentration profiles at the different heights collapse to single curves, indicating complete mixing within the enclosure, and the relative loss rates of helium from the enclosure decrease.

The effects of release location on the helium distributions within the enclosure for the four hour releases can be discerned by comparing time behaviors for the helium concentration profiles shown in Figure 4 for releases into the enclosure with a 3.05 cm square vent at locations at the lower rear and upper center of the enclosure with the corresponding profiles shown in Figure 3 (right). The two sets of concentration profiles for releases near the floor are seen to be very similar. Detailed comparisons show that at the ends of the release periods helium concentrations are slightly lower (< 1 % for all

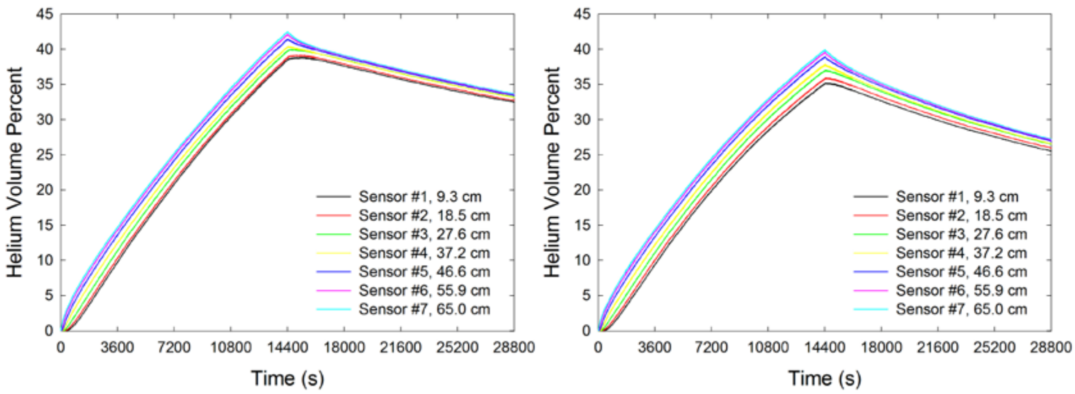

Figure 3. Helium volume fractions at seven heights plotted as a function of time for four hour releases at the center near the floor into enclosures with single 2.40 cm (left) and 3.05 cm (right) square vents.

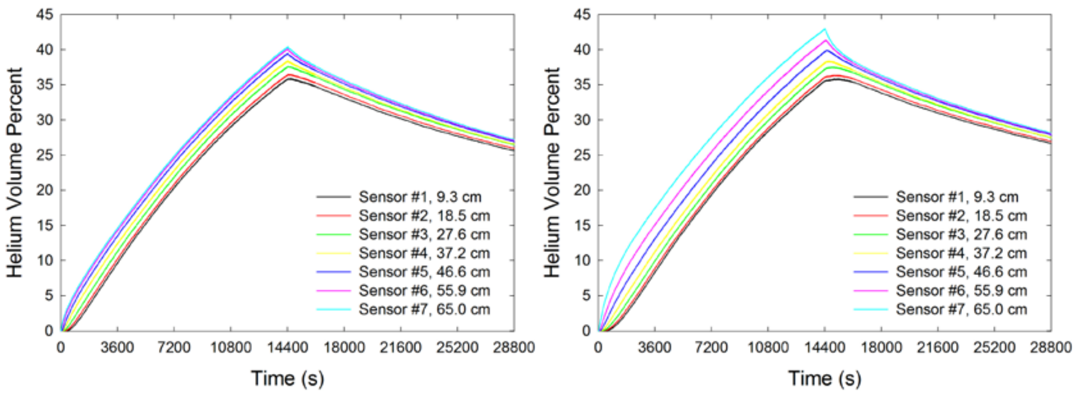

Figure 4. Helium volume fractions at seven heights plotted as function of time for four hour releases at the rear near the floor (left) and center near the ceiling (right) with 3.05 cm square vent.

heights) when the helium is released at the rear of the enclosure. In contrast, the concentration profiles for the release point located 2.5 cm below the center of the ceiling differ noticeably from those for the releases near the floor. The maximum concentration observed for the highest sensor (# 7) is increased by roughly 8 %, and the concentration gradients along the vertical direction are increased when the helium is released near the ceiling. The concentration variations immediately following the end of the release period are more accentuated for the upper release, with concentrations near the ceiling initially dropping and those closer to the floor continuing to increase for substantial periods following the end of the release. The concentrations for the upper release remain higher four hours after the end of the helium release, even though the concentration gradients appear to be similar.

The largest effects on mixing behavior were observed when the vent configuration was changed from a single opening at the center of the front face to two openings near the top and bottom. Figure 5 shows two sets of temporal curves for the seven sensors and four hour releases near the center of the floor (left) and near the ceiling (right) with two 2.15 cm square vents located near the top and bottom of the front face. The effect of vent location is best characterized by comparison with the right hand figures in Figures 3 and 4, which show the corresponding plots for four hour releases with a single vent of roughly the same total area. For the cases with upper and lower vents the maximum helium concentrations are significantly reduced, and the relative variations with height are much greater. Unlike for the releases with a single vent which are still rising at the end of the four hour release, the helium concentrations in the enclosure with two vents have nearly reached a steady state that begins to

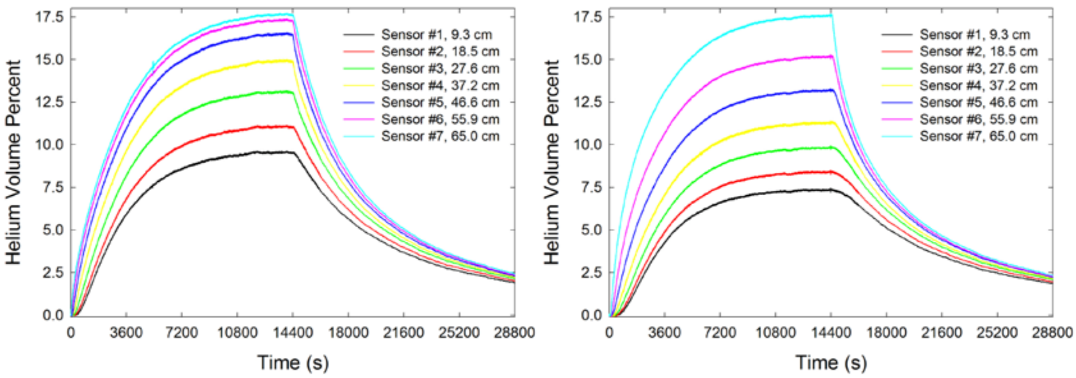

Figure 5. Helium volume fractions at seven heights plotted as function of time for four hour releases near the center of the floor (left) and ceiling (right) with two 2.15 cm square vents.

develop after roughly two hours. During the post release periods the helium concentrations fall much more rapidly for the cases with two vents. These increased exchange rates between the enclosure interior and surroundings for the two vent cases are due to the much larger hydrostatic pressure differences that are created by the density differences between the widely separated vents, that is buoyancy-induced ventilation.

Reducing the release time by a factor of 4 also has a strong effect on the concentration profiles at the seven heights. Figure 6 compares temporal concentration profiles for one hour and four hour releases for a single 3.05 cm square vent and two 2.15 cm square vents for helium releases at the center of the enclosure near the floor and near the ceiling. As expected, higher concentrations are observed for the one hour releases. The highest concentrations observed were for the one hour release near the ceiling with a single vent. With the single vent and release near the floor the concentration gradients are similar for the two release periods. When the helium is released near the ceiling it tends to accumulate more in this area for the one hour release, and the concentration gradients are larger and the concentration profiles change more dramatically at the end of the release. Similar comments apply to the two sets of curves for the two vent front face, but the differences between the one hour and four hour releases are much greater, and the concentration profiles have very different shapes. All of the concentration profiles are continuing to increase at the end of the one hour release, while they are approaching steady states for the four hour releases. With two vents the maximum concentrations for the one hour and four hour releases differ by roughly a factor 2, but are comparable for releases near the floor and ceiling. For this vent configuration larger concentration gradients are generated for the upper release as compared to release near the floor.

Figure 7 compares measured temporal helium concentration profiles with the corresponding predictions from FDS for releases from the center of the enclosure near the floor for cases with a single 2.4 cm square vent and with the upper and lower 2.15 cm square vents in the front wall. For all of the profiles differences between the calculations and measurements are less than 10 % and are generally much less. The calculations capture the effects of the differences in vent arrangement on helium concentrations, vertical gradients, and losses during the post release period very well. The largest differences are observed for the two vent case. This is not surprising since hydrostatic pressure differences induce flows that dominate the flow into and out of the enclosure. The fidelity with which the vent effects are captured is crucial. The observed agreement between the calculations and measurements indicates FDS is reproducing these flows well. It is considered likely that improved quantitative agreement can be obtained by higher resolution gridding near the vents. Since an unmodified production version of FDS was used, we conclude that use of the unmodified FDS code is

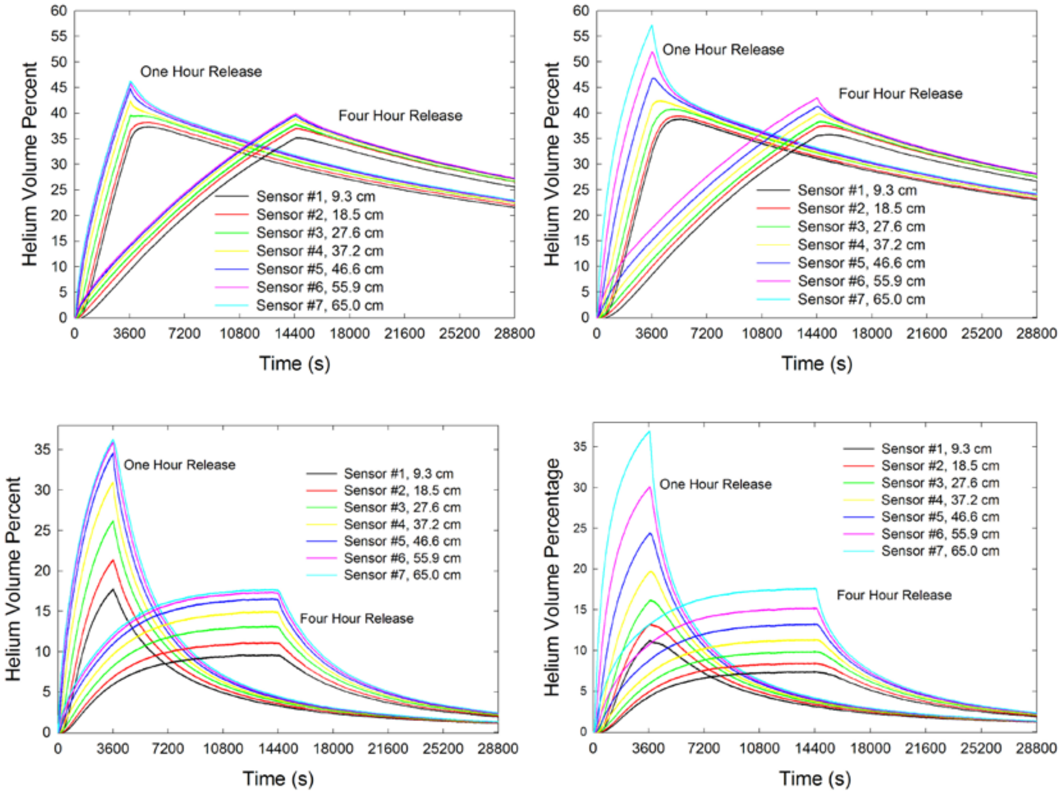

Figure 6. Helium concentration time behaviors at the seven vertical locations are compared for one hour and four hour releases for center releases near the floor (left) and ceiling (right) with a single 3.05 cm square vent (top) and two 2.05 cm square vents (bottom), respectively.

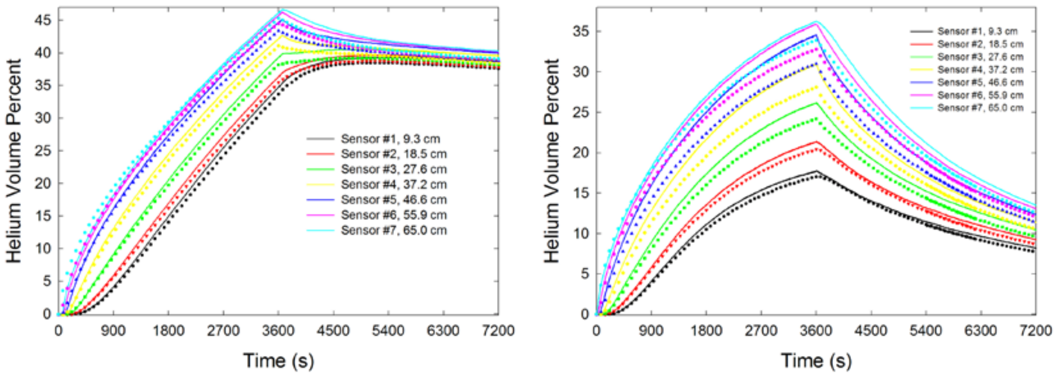

Figure 7. Results of measurements (lines) of helium concentration at seven heights for one hour helium releases at the center of the enclosure near the floor with a single 2.4 cm vent (left) and upper and lower 2.15 cm square vents (right) are compared with predicted results (symbols) from FDS.

appropriate for predicting the dispersion of highly buoyant gases within an enclosure as well as the loss of the gases from the enclosure.

4. SUMMARY

Experimental results have been summarized for the dispersion of released helium within an enclosure representing a ¼-scale model of a two car garage. A particular focus has been the effect of transport of helium from the enclosure to the surroundings. Parameters varied include release rate, release location, vent size, and number of vents and locations. The helium distribution within the enclosure was most sensitive to the vent location, with the presence of two vents near the top and bottom of the wall providing the most efficient removal of helium from the enclosure. This finding is consistent with the modeling of Barley et al. [16]

An internal report is in preparation that will include an appendix with tables of experimental results for each of the 18 cases considered during this study. It is hoped that the results will prove useful to the research community for modeling and validation of CFD codes. The NIST CFD model FDS has been shown to be effective for predicting the experimental behaviors without modification. These findings suggest that FDS can be confidently used to predict similar enclosure flows involving hydrogen.

---

1. Koontz, M.D., Burruss, R., Cade, D.R. and Rector, H.E., Hydrogen Emissions from Electric Vehicle Batteries Undergoing Charges in Residential Garages, Electric Power Research Institute Technical Report 103421, 1993.
2. Swain, M.R., Shriber J. and Swain, M.R., Comparisons of Hydrogen, Natural Gas, Liquified Petroleum Gas, and Gasoline Leakage in a Residential Garage, *Energy and Fuels*, **12**, No. 1, 1998, pp. 83-89.
3. Swain, M.R., Grilliot, E.S., Swain, M.N., The Application of a Hydrogen Risk Assessment Method to Vented Spaces, Advances in Hydrogen Energy (Gregoire Padro, C.E., Lau, F. Eds.), Kluwer Academic Publishers, Hingham, MA, 2000, pp. 163-173.
4. Swain, M.R., Filoso, P., Grilliot, E.S. and Swain, M.N., Hydrogen Leakage into Simple Geometric Enclosures, International Journal of Hydrogen Engineering, **28**, No. 2, 2003, pp. 229-248.
5. Swain, M.R., Addendum to Hydrogen Vehicle Safety Report: Residential Garage Safety Assessment, Directed Technologies, Inc., Arlington, VA, August 1998.
6. Papanikolaou, E.A. and Venetsanos, A.G., CFD Modeling for Helium Releases in a Private Garage without Forced Ventilation, First International Conference on Hydrogen Safety, 8-10 September 2005, Pisa, Italy.
7. Breitung, W., Necker, G., Kaup, B and Veser, A., Numerical Simulation of Hydrogen Release in a Private Garage, Proceedings of the 4th International Symposium on Hydrogen Power - Theoretical and Engineering Solutions, 9-14 September 2001, Strahlsund, Germany, pp. 368-377.
8. Gallego, E., Migoya, E., Martin-Valdepenas, J.M., Crespo, A., Garcia, J., Venetsanos, A., Papanikolaou, E., Kumar, S., Studer, E., Dagba, Y., Jordan, T., Jahn, W., Hoiset, S., Makarov, D. and Piechna, J., An Intercomparison Exercise on the Capabilities of CFD Models to Predict Distribution and Mixing of H_2 in a Closed Vessel, *International Journal of Hydrogen Energy*, **32**, No. 13, 2007, pp. 2235-2245.
9. Shebeko, Y.N., Keller, V.D., Yeremenko, O.Y., Smolin, I.M., Serkin, M.A., Korolchenko, A.Y., Regularities of Formation and Combustion of Local Hydrogen-Air Mixtures in a Large Volume, Chemical Industry, **24**, 1988, pp. 728-731 (in Russian).
10. Gupta, S., Brinster, J., Studer, E. and Tkatschenko, I., Hydrogen Related Risks within a Private Garage: Concentration Measurements in a Realistic Full Scale Experimental Facility, Second International Conference on Hydrogen Safety, 11-13 September 2007, San Sebastian, Spain.

11. Lacome, J.M., Dagba, Y., Jamois, D., Perrette, L. and Proust, Ch., Large-Scale Hydrogen Release in an Isothermal Confined Area, Second International Conference on Hydrogen Safety, 11-13 September 2007, San Sebastian, Spain.
12. Tchouvelev, A.V., DeVaal, J., Cheng, Z., Corfu, R., Rozek, R. and Lee, C., CFD Modeling of Hydrogen Dispersion Experiments for SAE J2578 Test Method Development, Second International Conference on Hydrogen Safety, 11-13 September 2007, San Sebastian, Spain.
13. Ishimoto, Y., Merilo, E., Groethe, M., Chiba, S., Iwabuchi, H. and Sakata, K., Study of Hydrogen Diffusion and Deflagration in a Closed System, Second International Conference on Hydrogen Safety, 11-13 September 2007, San Sebastian, Spain.
14. Venetsanos, A.G., Papanikolaou, E., Delichatsios, M., Garcia, J., Hansen, O.R., Heitsch, M., Huser, A., Jahn, W., Jordan, T., Lacome, J-M., Ledin, H.S., Makarov, D., Middha, P., Studer, E., Tchouvelev, A.V., Teodorczyk, A., Verbecke, F. and van der Voort, M.M., An Inter-Comparison Exercise on the Capabilities of CFD Models to Predict the Short and Long Term Distribution and Mixing of Hydrogen in a Garage, International Journal of Hydrogen, 2009, accepted for publication.
15. Zhang, J, Hereid, J., Hagen, M., Bakirtzis, D., Delichatsios, M.A. and Venetsanos, A.G., Numerical Studies of Dispersion and Flammable Volume of Hydrogen in Enclosures, Second International Conference on Hydrogen Safety, 11-13 September 2007, San Sebastian, Spain.
16. Barley, C.D., Gawlik, K., Ohi, J. and Hewett, R., Analysis of Buoyancy-Driven Ventilation of Hydrogen from Buildings, Second International Conference on Hydrogen Safety, 11-13 September 2007, San Sebastian, Spain.
17. McGrattan, K., Hostikka, S., Floyd, J., Baum, H., Rehm, R., and McDermott, R., Fire Dynamics Simulator (Version 5) Technical Reference Guide, Special Publication 1018-5, National Institute of Standards and Technology, Gaithersburg, MD, October 2007.
18. Sherman, M.H. and Chan, R., Building Airtightness: Research and Practice, Report LBNL-53356, Lawrence Berkeley National Laboratory, Livermore, CA, 2003.
19. Emmerich, S.J., Gorfain, J.E., Huang, M. and Howard-Reed, C., Air and Pollutant Transport from Attached Garages to Residential Living Spaces, Internal Report 7072, National Institute of Standards and Technology, Gaithersburg, MD, December 2003.
20. Ventilation for Acceptable Indoor Air Quality, ANSI/ASHRAE Standard 62-1989, American Society of Heating, Refrigeration, and Air Conditioning Engineers, Atlanta, GA, 1990.
21. International Mechanical Code, International Code Council, Inc., Country Club Hills, IL, 2009.
22. Mulholland, G. and Fernandez, M., Report on the Calibration of the Gilibrator-2 Soap Film Flowmeter, Unpublished Report, National Institute of Standards and Technology, 24 February 1997.
23. Chen, C.J. and Rodi, W., Vertical Turbulent Buoyant Jets—A Review of Experimental Data, 1980, Pergamon Press, Oxford.
24. Pitts, W.M., Mulholland, G.W. Breuel, B.D., Johnsson, E.L., Chung, S., Harris, R. and Hess, D.E., Real-Time Suppressant Concentration Measurement, Gann, R.G., ed., Fire Suppression System Performance of Alternative Agents in Aircraft Engine and Dry Bay Laboratory Simulations, Vol. II, Special Publication 890, National Institute of Standards and Technology, pp. 319-585, 1995.
25. Prasad, K., Pitts, W.M. and Yang, J.C., A Numerical Study of Hydrogen or Helium Release and Mixing in Partially Confined Spaces, Conference and Hydrogen Expo, National Hydrogen Association, 30 March – 3 April 2009, Columbia SC.